Int. J. Environ. Sci. Technol. (2014) 11:1537–1548
DOI 10.1007/s13762-013-0295-z

ORIGINAL PAPER

Nitric oxide absorption by hydrogen peroxide in airlift reactor: a study using response surface methodology

A. D. Bhanarkar · R. K. Gupta · R. B. Biniwale · S. M. Tamhane

Received: 10 January 2012 / Revised: 28 March 2012 / Accepted: 23 April 2013 / Published online: 17 May 2013

Abstract Absorption of nitric oxide from nitric oxide /air mixture in hydrogen peroxide solution has been studied on bench scale internal loop airlift reactor. The objective of this investigation was to study the performance of nitric oxide absorption in hydrogen peroxide solution in the airlift reactor and to explore/determine the optimum conditions using response surface methodology. A Box–Behnken model has been employed as an experimental design. The effect of three independent variables—namely nitric oxide gas velocity, 0.02–0.11 m/s; nitric oxide gas concentration, 300–3,000 ppm and hydrogen peroxide concentration, 0.25–2.5 %—has been studied on the absorption of nitric oxide in aqueous hydrogen peroxide in the semi-batch mode of experiments. The optimal conditions for parameters were found to be nitric oxide gas velocity, 0.02 m/s; nitric oxide gas concentration, 2,246 ppm and hydrogen peroxide concentration, 2.1 %. Under these conditions, the experimental nitric oxide absorption efficiency was observed to be ∼65 %. The proposed model equation using response surface methodology has shown good agreement with the experimental data, with a correlation coefficient (R^2) of 0.983. The results showed that optimised conditions could be used for the efficient absorption of nitric oxide in the flue gas emanating from industries.

Keywords Nitric oxide absorption · Response surface methodology · Box–Behnken experimental design · Hydrogen peroxide · Optimisation

Introduction

It is difficult to obtain the significant NO_x removal efficiency because of the low solubility of nitric oxide (NO) that accounts for more than 90 % of all oxides of nitrogen as NO_x (Jin et al. 2006; Long et al. 2008) by wet removal processes. Several authors have studied the use of various aqueous solutions (acid urea, hydrogen peroxide, sodium hypochlorite, sodium sulphite solutions, etc.) for the removal of NO_x (Kasper et al. 1996) in waste gases, discharged from nitric acid towers, power plants, steel pickling plants and organic process plants. The oxidising process using aqueous hydrogen peroxide (H_2O_2) as absorbing media appears to be suited for control of tail gas NO_x emissions from various sources, having basic advantage of NO oxidation to NO_2 and generation of nitric acid for eventual reuse in the system (Thomas and Vanderschuren 1997, 1998).

In absorption-based methods, it is desirable to have knowledge of the process variables and their influence on absorption capacity to maximise removal efficiency of the contaminants in pre-decided absorbents. The conventional approach for optimisation of process variables involves many experiments to be performed, which otherwise would be expensive and time-consuming. Moreover, it does not reveal the influence of the interactions between the process variables on the dependent variable (Moghaddam et al. 2011). Response surface methodology (RSM) has been applied to optimise and evaluate interactive effects of independent factors in numerous chemical and biochemical

A. D. Bhanarkar · R. K. Gupta · S. M. Tamhane
Air Pollution Control Division, National Environmental Engineering Research Institute, (Council of Scientific and Industrial Research), Nehru Marg, Nagpur 440 020, India

R. B. Biniwale (✉)
Environmental Materials Division, National Environmental Engineering Research Institute, (Council of Scientific and Industrial Research), Nehru Marg, Nagpur 440 020, India
e-mail: rb_biniwale@neeri.res.in

processes. Recently, several studies describe the use of RSM in various fields such as in biochemistry for fermentation medium optimisation (Martendal et al. 2007; Murthy et al. 2000), in material processing for describing the performance of coated carbide tools and concrete production (Kockal and Ozturan 2011; Noordin et al. 2004), in pharmaceutical industry for determining influences of parameters on formulation of physical properties on nasal spray (Guo et al. 2008) and in water treatment for studying the optimisation of the coagulation flocculation processes (Ahmad et al. 2005). The application of RSM technique on optimising the NO absorption has been envisage their study.

In the present study, the investigation propose to use an airlift reactor (ALR) which is modified bubble column with draft tube to enhance liquid circulation by internal or external loop. Difference in gas hold-up and bulk densities in riser and downcomer sections of ALR cause liquid circulation flow in an ALR (Fadavi and Chisti 2005). It is widely used in gas absorption, chemical and biochemical processes. Recently, much attention has been paid to ALRs because of the many advantages such as simple construction, no moving parts, better mixing, faster gas transfer rates, low shear stresses, low power requirements and relatively homogeneous flow pattern (Jia et al. 2006).

The objective of the present study was to investigate the NO absorption using different concentrations of aqueous H_2O_2 solutions and to find the optimum conditions for an efficient NO removal in a bench scale internal loop ALR. The Box–Behnken design has been applied in the optimisation of experiments using RSM to understand the effect of various operating parameters and their interactions on NO absorption efficiency. The optimum values of the parameters have been determined for NO absorption.

Materials and methods

Materials and instruments

Analytical reagent grade H_2O_2 (30 %, w/v; Merck, India) was used in the preparation of absorbing media. Different concentrations of absorbing media were prepared by dissolving the desired amount of H_2O_2 in deionised water (Millipore, Milli-Q, USA). A standard mixture of NO gas (49.28 % v/v; Alchemie Gases & Chemicals, India) balance nitrogen was used. Flow of NO and air was controlled with the help of mass flow controllers (McMillan, 80-SD, USA) and rotameters, respectively. Gas analyser (Testo, 350-S, Germany) was calibrated in the experimental range and used for measurement of NO concentration. This analyser is portable extractive electrochemical sensor-based gas analyser, which provides continuous measurements over long duration.

Experimental

Figure 1 shows schematic diagram of a bench scale internal loop ALR assembly for NO gas absorption. A reactor comprises of two cylindrical perspex columns. The overall height of the reactor was 2.35 m; height of outer column was 1.71 m with internal diameter 0.098 m. The height of draft tube was 1.05 m, and internal diameter was 0.072 m. The column is equipped pressure taps at annulus and riser region for the measurement of pressure drop. The circular perforated air sparger having 1-mm holes in concentric circle with pitch of 5 mm was employed. The mixture of NO and air at atmospheric pressure and room temperature (30 °C) was fed in ALR column for NO absorption. Different NO concentrations were fed to ALR by mixing the gas with compressed air in different ratios. The inlet and outlet concentration of NO were monitored by the gas analyser. The concentration measurements were taken continuously at every 1-min interval. NO sensor works according to the electrochemical principle of ion selective potentiometry. Concentration of NO is determined in terms of current flow in external circuit generated from chemical reactions occur with the aid of oxygen from fresh air at the counter electrode where H^+ ions are migrating from sensing electrode. H^+ ions are formed as a result of chemical reaction that takes place when the NO molecule pass through the gas-permeable membrane to sensing electrode of the sensor filled with an aqueous electrolytic solution. The reference electrode is used to stabilise the sensor signal.

The per cent NO removal was calculated for each run by following expression:

$$\%\ \text{NO removal} = \frac{C_i - C_f}{C_i} \times 100 \quad (1)$$

where C_i (ppm) is the initial or inlet concentration, and C_f (ppm) is the final or outlet concentration. All the experiments were run for 120 min.

Response surface methodology

Response surface methodology (RSM) is a collection of mathematical and statistical techniques that are useful for developing, improving and optimising processes and can be used to evaluate the relative significance of several parameters and their effects even in the presence of complex interactions. RSM involves the following advantages: (1) it provides more information on the experiment than unplanned approaches; (2) it reduces number and cost of experiments; (3) it makes possible to study the interactions

Fig. 1 Schematic diagram of NO absorption in airlift reactor

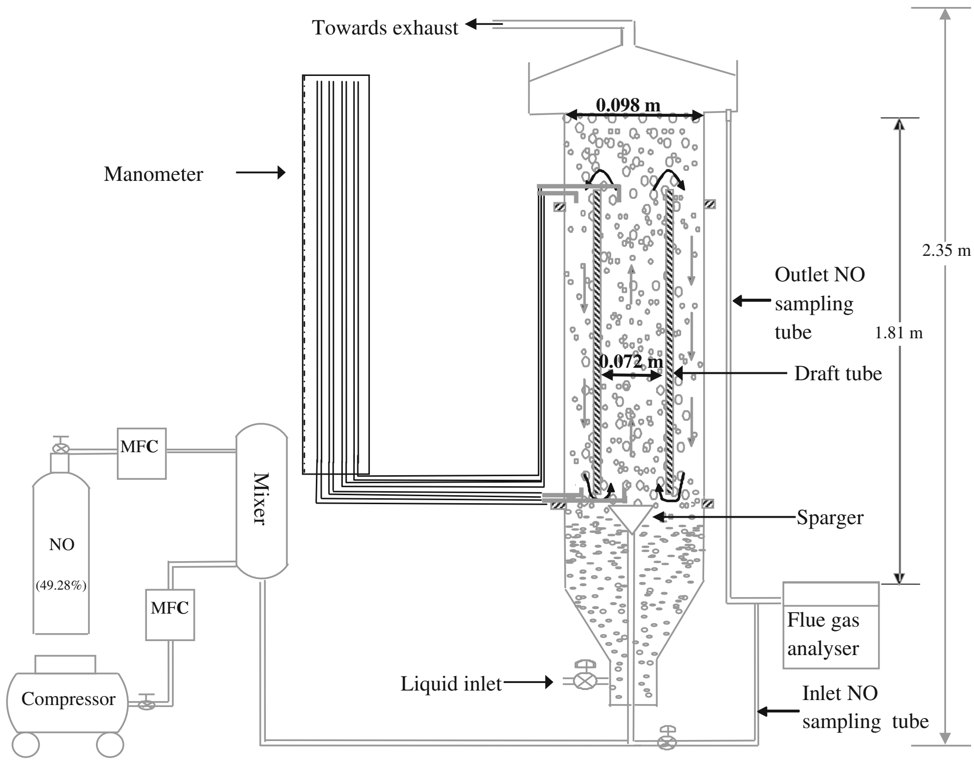

among experimental variables within the range studied, leading to a better understanding of the process; and (4) it facilitates to determine operating conditions necessary for the scale-up of the process. Its greatest applications have been in industrial research, particularly in situations where most of variables influencing the system feature (Montgomery 1996; Myers and Montgomery 2002).

The Box–Behnken design optimises the number of experiments to be carried out to ascertain the possible interactions between the parameters studied and their effects on the absorption of NO. Box–Behnken design is a spherical, revolving design; it consists of a central point and the middle points of the edges of the cube circumscribed on the sphere (Evans 2003).

Experimental design for absorption studies

In order to obtain the optimum condition for NO absorption, three independent parameters were selected based on the literature available. These are presented in Table 1. The operating ranges for NO gas velocity (X_1), initial NO concentration (X_2) and H_2O_2 concentration (X_3) were determined by an iterative method. Initially, a few preliminary experiments were carried out using the range of variables from 0.06 to 0.15 m/s, 300 to 3,000 ppm and 1 to 5 % for X_1, X_2 and X_3, respectively. The final range of parameters was determined from analysis of the data by plotting contour graphs indicating maxima and minima on the entire range. In the case of velocity and H_2O_2 concentration, finer region of interest was selected by narrowing the range of variables. The relationship between the parameters and response was determined using Box–Behnken design under RSM. In this study, the experimental plan consisted of 15 trials, and the independent variables were studied at three different levels, low (−1), medium (0) and high (+1). A Box–Behnken experimental design has the advantage of requiring fewer experiments (15 batches) than that would require in a full factorial design (27 batches). Box–Behnken design presents an approximately rotatable design with only three levels per variable and combines a fractional factorial with incomplete block design excluding the extreme vertices. The Box–Behnken design has good performance with less error. The percentage of NO removal is taken as a response (Y) of the experimental design.

In the optimisation process, the responses can be simply related to chosen variables by linear or quadratic models. A quadratic model, which also includes the linear model, is given below:

$$Y = \beta_0 + \sum_{i=1}^{k} \beta_i x_i + \sum_{i=1}^{k} \beta_{ii} x_i^2 + \sum_{i=1}^{k} \sum_{j=1}^{k} \beta_{ij} x_i x_j + \varepsilon \tag{2}$$

where Y is the response and $x_1, x_2, \ldots, x_k$ are the coded independent variables, β_i, β_j and β_{ij} are the linear, quadratic and interaction coefficients, respectively. β_0 and ε are the constant and the random error, respectively.

Table 1 Experimental range and levels of variables

Variables	Code	Unit	Range and levels			
			Low level (−1)	Centre level (0)	High level (+1)	Step change (ΔX_i)
Gas velocity	X_1	(m/s)	0.02	0.065	0.11	0.045
Gas concentration	X_2	(ppm v/v)	300	1,650	3,000	1,350
H_2O_2 concentration	X_3	(% w/v)	0.25	1.35	2.5	1.1

Statistical analysis

The significance of the independent variables and their interactions was tested by the analysis of variance (ANOVA). Results were assessed with various descriptive statistics such as t ratio, p value, F value, degrees of freedom (df), coefficient of variation (CV), correlation coefficient (R^2), adjusted correlation coefficient (R^2_{adj}), sum of squares (SS), mean sum of squares (MSS), Mallow's C_p statistic and chi-square (χ^2) test to reflect the statistical significance of the quadratic model. The standardised effects of the independent variables and their interactions on the dependent variable were also analysed by preparing a Pareto chart. For the validation of the quadratic model, a nonparametric Mann–Whitney U test and a parametric two-sample (unpaired) t test were conducted to evaluate the relationship between the validation data and the corresponding model predicted responses. The Design-Expert (trial version 8.0.5, Stat-Ease Inc., USA) software package was used for regression analysis of experimental data, and to plot response surface.

Validation experiments

The mathematical model generated during RSM implementation was validated by conducting additional experiments for different combinations of the three independent variables in a random fashion, each within its respective experimental range.

Results and discussion

Statistical evaluation

In order to study the effects of three independent variables on the absorption efficiency of NO, semi-batch runs were conducted at different combinations of the process parameters using Box–Behnken designed experiments. The NO gas concentration range studied was between 300 to 3,000 ppm. The gas velocity varied between 0.02 and 0.11 m/s. The concentration of H_2O_2 solution kept between 0.25 and 2.5 %. Table 2 contains the results along with the experimental conditions. By applying multiple regression analysis on the design matrix and the responses given in Table 2, established approximate function for absorption efficiency applicable for reactor in the present study in uncoded form is given in Eq. (3)

$$Y = 17.8467 - 308.32X_1 + 0.0209X_2 + 28.1032X_3 + 940.535X_1^2 - 4.93 \times 10^{-6}X_2^2 - 6.1554X_3^2 + 2.8 \times 10^{-2}X_1X_2 - 76.59X_1X_3 + 7.9 \times 10^{-4}X_2X_3 \quad (3)$$

where Y is the NO absorption efficiency, X_1, X_2 and X_3 are corresponding uncoded variables of NO gas velocity, gas concentration and H_2O_2 concentration, respectively.

The summary of ANOVA of the regression model presented in Table 3 indicates that the model equation can adequately be used to describe the absorption of NO under a wide range of operating conditions. F value of 33.11 which was found to be greater than the tabulated value ($F_{\mathrm{tab}} = 4.1$) implies that the model is significant for absorption of NO. For the fixed model, adequate precision can be ensured with a signal-to-noise ratio >4. An adequate precision of 20.04 suggests the ability of model to precisely navigate through the design space. The low probability value (p model $> F = 0.0006$) <0.05 indicates quadratic model is highly significant.

The goodness of fit of the model was checked by calculating the regression coefficient (R^2). A fairly high value of R^2 (0.983) suggests that most of the data variation was explained by the regression model. Moreover, a closely high value of the adjusted regression coefficient ($R^2_{\mathrm{adj}} = 0.954$) indicates the capability of the developed model to satisfactorily describe the system behaviour within the studied range of operating parameters, as similarly reported by others (Can et al. 2006). According to the literature, R^2_{adj} corrects R^2 for the sample size and the number of terms in the model; for example, many terms in the model and small sample size might cause that $R^2_{\mathrm{adj}} << R^2$, which is not obtained in our study. A similar pattern has been reported by others for the second-order RSM experiments based on Box–Behnken (Khajeh 2011) and central composite (Liu et al. 2004) designs. Further, a relatively low value of the coefficient of variation (CV = 7.92 %) indicates good precision and reliability of the conducted experiments.

Table 2 Box–Behnken experimental design matrix with variables and NO absorption

Run order	Coded variables			Uncoded variables			Response
	x_1	x_2	x_3	Gas velocity (m/s)	Gas conc. (ppm)	H_2O_2 conc. (%)	Observed NO absorption efficiency (%)
1	0	0	0	0.065	1,650	1.38	48
2	0	1	1	0.02	3,000	2.50	51.3
3	−1	0	−1	0.065	1,650	0.25	39.74
4	0	1	−1	0.02	3,000	0.25	35
5	−1	1	0	0.11	3,000	1.38	57.77
6	1	0	−1	0.11	1,650	0.25	24.3
7	1	1	0	0.065	3,000	1.38	40.3
8	0	0	0	0.11	1,650	1.38	47.3
9	1	0	1	0.065	1,650	2.50	36.4
10	0	−1	−1	0.02	300	0.25	13.2
11	−1	−1	0	0.11	300	1.38	44.61
12	1	−1	0	0.065	300	1.38	20.3
13	0	0	0	0.02	1,650	1.38	48.2
14	−1	0	1	0.065	1,650	2.50	67.35
15	0	−1	1	0.065	300	2.50	24.7

Table 3 Analysis of variance (ANOVA) of the response surface quadratic model for the prediction of NO absorption efficiency

Factor (coded)	Sum of squares	*DF*	Mean square	*F* value	*p* value	Remark
Model	2,972.27	9	330.3	33.11	0.0006	Significant
x_1	971.74	1	971.7	97.43	0.0002	Significant
x_2	831.50	1	831.5	83.37	0.0003	Significant
x_3	569.70	1	569.7	57.12	0.0006	Significant
x_1^2	13.39	1	13.4	1.34	0.2988	
x_2^2	298.61	1	298.6	29.94	0.0028	Significant
x_3^2	224.09	1	224.1	22.47	0.0051	Significant
x_1x_2	11.70	1	11.7	1.17	0.3283	
x_1x_3	60.14	1	60.1	6.03	0.0575	
x_2x_3	5.76	1	5.8	0.58	0.4816	
Residual	49.87	5	10.0			
Lack of fit	49.42	3	16.5	73.76	0.0134	Significant
Pure error	0.45[a]	2	0.2[b]			
Cor. total	3,022.14	14				

DF degrees of freedom

[a] SS_E

[b] MSS_E

The χ^2 test was also carried out to check whether there was a significant difference between the expected responses and the observed data. The calculated χ^2 value ($\chi^2_{cal} = 1.59$) was found to be less than the tabulated value ($\chi^2_{tab} = 23.69$), suggesting that there was insignificant difference between the observed and the expected responses. The χ^2 test concluded with 95 % certainty that the quadratic model provided a satisfactory fit to the experimental data.

The diagnostic plots shown in Fig. 2 were used to estimate the adequacy of the regression model. Figure 2a shows the experimental and the predicted NO absorption. The observed and predicted values of NO absorption efficiency are in well agreement. The points cluster around the diagonal line indicates a good fit of the model. The normal probability of the residuals (Fig. 2b) suggests almost no serious violation of the assumptions underlying the analysis, and it confirmed the normality assumptions and independence of the residuals. Moreover, the comparison of the residuals with the error variance showed that none of the individual residual exceeded the value twice of the square root of the error variance. The plot presented in Fig. 2c tests the assumption of constant variance. The points are randomly scattered, and all values are lying within the range of −2.15 and 2.15 (values beyond −3 and +3 are considered as the top and bottom outlier detection limits). Accordingly, it was inferred that developed quadratic equation was appropriate and is successful in capturing the correlation between the influencing parameters of NO absorption process.

Mallow's C_p statistic can be used to determine terms which can be omitted from the response surface model. For a response surface model including all terms, $C_p = p$, where p is the number of variables in the regression model including the intercept term. For response surface models with omitted terms, $C_p \sim p$ shows a good model with little bias and $C_p \leq p$ shows a very good prediction model. The goal is to remove terms from the response surface model until a minimum C_p value near p is obtained. If $C_p > p$, this shows that too many terms have been removed or some remaining terms are not necessary. In this study, Mallow's C_p statistic ($C_p = 9.99$) showed the third condition ($C_p \leq p$ and $p = 10$), indicating a very good prediction model, as similarly reported by others (Khajeh 2011).

Effect of model components and their interactions on NO absorption

The results of Student's t test and p values conducted to evaluate the significance of the quadratic model coefficients are listed in Table 4. Results showed that all the linear and quadratic (except NO gas concentration, X_2 and H_2O_2 concentration, X_3) terms are statistically significant ($p < 0.05$). All interactive terms were found statistically insignificant. Moreover, the first-order main effects of all the three independent variables, namely NO gas velocity (x_1), gas concentration (x_2) and H_2O_2 concentration (x_3), were found to be more significant than their respective quadratic effects (x_1^2, x_2^2 and x_3^2). The t and p value (Tables 3, 4) suggest that the NO gas velocity, gas concentration and H_2O_2 concentration have a direct relationship on the NO absorption efficiency. NO gas velocity was found to be the most significant component of the regression model for the present application, whereas the interaction term between NO concentration and H_2O_2 concentration showed the lowest effect on the NO absorption efficiency.

Figure 3 shows Pareto chart depicting the standardised effects of the independent variables and their interactions on the dependent variable. It was noted that the bar for X_1X_3, X_1X_2, X_2X_3, X_2^2 and X_3^2 remained inside the reference line (p-0.05) in Fig. 3, and the smaller coefficients for these terms compared to other terms in Eq. (3), implies that these terms contributed the least in prediction of the NO absorption efficiency. The NO gas velocity (X_1), and its interactive terms with H_2O_2 concentration (X_1X_3), along with the quadratic terms of gas concentration (X_2^2) and H_2O_2 concentration (X_3^2) exhibited a negative relationship with the NO absorption process, whereas the NO gas concentration (X_2) and H_2O_2 concentration (X_3) along with the quadratic term of NO gas velocity (X_1^2) and interaction terms of NO gas concentration with gas velocity (X_1X_2) and H_2O_2 concentration (X_2X_3) showed a positive significant effect on the process.

Table 4 also includes the per cent contribution (PC) of each of the individual terms in the final model computed using the sum of squares (SS) values of the corresponding term. As evident from Table 4, the NO gas velocity (X_1) showed the highest level of significance with a contribution of >32 % as compared to other components. Results revealed that among the calculated Total Percent Contribution (TPC) values, first-order terms had the highest level of significance with a total contribution of 79.45 % as compared to other TPC values. This was followed by the TPC of quadratic terms with a total contribution of 17.95 %. The TPC of interaction terms showed the lowest level of significance with a total contribution of 2.60 %, indicating that the interaction components showed a little effect in prediction of the NO removal efficiency. Hence, TPC values also proved that the first-order independent variables have a direct relationship on the dependent variable.

Optimisation of experimental condition for NO absorption

In order to gain better understanding of the influence of the independent variables and their interactions on the dependent variable, 3D response surface plots for the measured responses were drawn based on the quadratic model. Figure 4 exhibits the 3D response surfaces plots as the functions of two independent variables keeping other variable fixed at the centre level. It can be seen from Fig. 4a

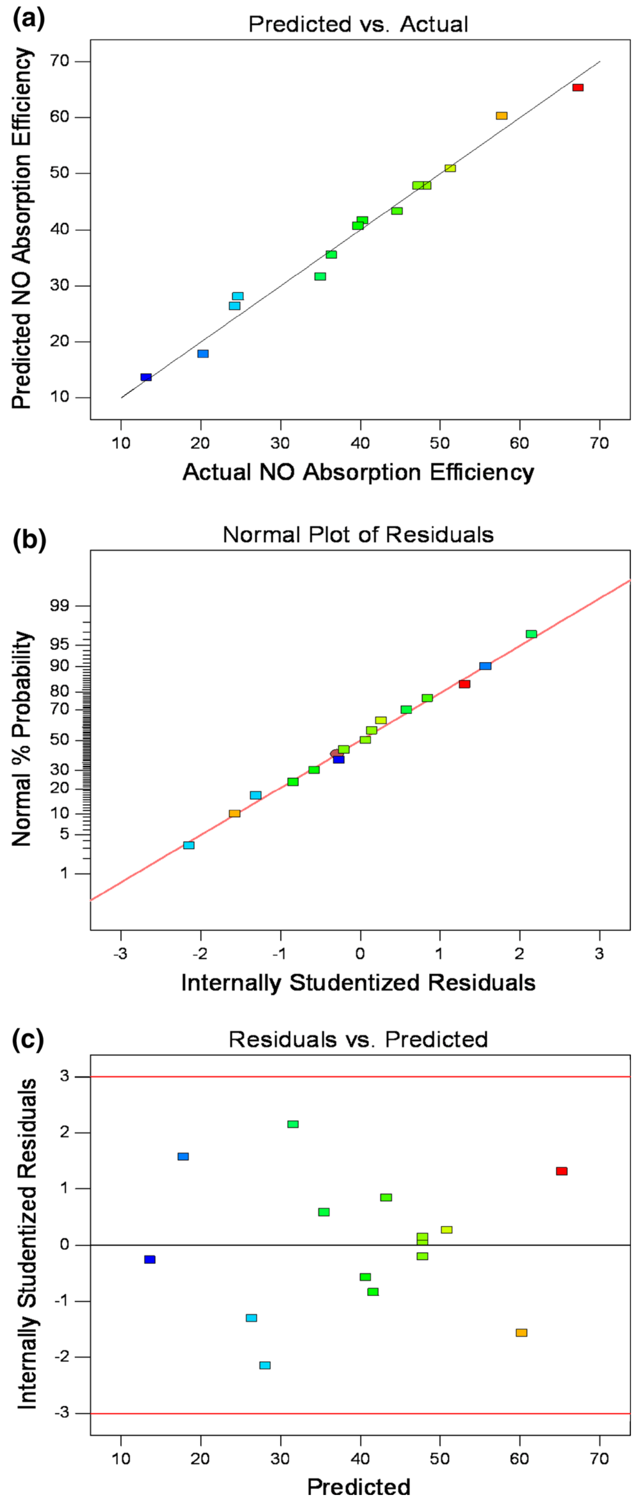

Fig. 2 **a** Plot of the measured and model predicted values of the response variable, **b** the normal probability plot of the raw residuals **c** the internally studentised residuals versus predicted values plot

Table 4 Multiple regression results and significance of the components for the quadratic model

Factor (coded)	Coefficient	Standard error	Effect	*t* ratio	PC (%)
Intercept	47.83	1.823	95.67		
x_1	−11.02	1.117	−22.04	−19.74	32.54
x_2	10.20	1.117	20.39	18.26	27.84
x_3	8.44	1.117	16.88	15.12	19.07
x_1^2	1.90	1.644	3.81	2.32	0.45
x_2^2	−8.99	1.644	−17.99	−10.94	10.00
x_3^2	−7.79	1.644	−15.58	−9.48	7.50
x_1x_2	1.71	1.579	3.42	2.17	0.39
x_1x_3	−3.88	1.579	−7.76	−4.91	2.02
x_2x_3	1.20	1.579	2.40	1.52	0.19

PC per cent contribution

that NO absorption efficiency increased with increasing NO concentration from 300 to 2,500 ppm and then slightly decreased with the increase in NO concentration, whereas the reverse trend was obtained in the case of influence of gas velocity on NO absorption efficiency. At higher gas concentration, the absorbing media get saturated within the experimental time frame which results in slight decrease in NO absorption. At low values of gas velocity, the gas hold-up increases relatively sharply with the increase in gas velocity. Similar behaviour of gas hold-up with superficial gas velocity has been reported by Han et al. (2005) and Mehrnia et al. (2005). In the region of lower gas velocities, an increase in gas velocity results in the formation of a large number of bubbles without appreciably increasing the bubble diameters. Therefore, at any section, the area

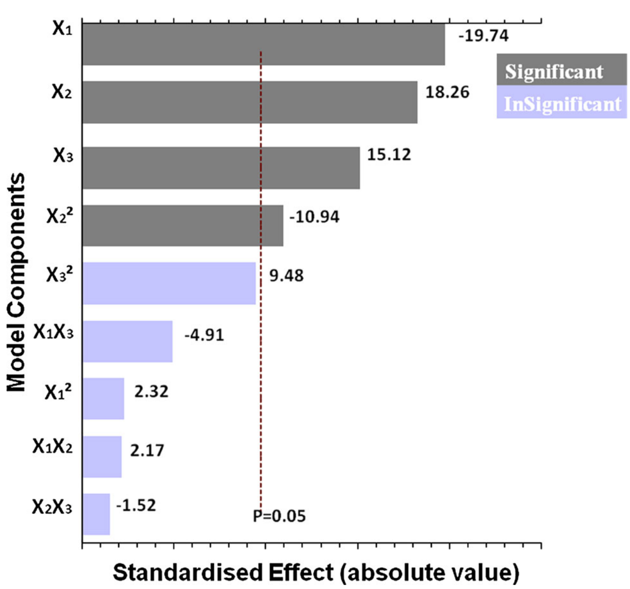

Fig. 3 Pareto chart showing standardised effect of independent variables and their interaction on NO absorption efficiency

occupied by the gas increases thereby increasing the gas hold-up. In the region of higher gas velocities, however, due to formation of larger bubbles and bubble coalescence, the rate of increase in gas hold-up with gas velocity slightly decreases. NO absorption efficiency decreased with increasing gas velocity (Paiva and Kachan 1998) from 0.02 to 0.11 m/s. A significant absorption was observed at NO concentration more than 700 ppm and gas velocity <0.06 m/s.

In theory, the increase in H_2O_2 concentration applied in the NO_x absorption process can be helpful to the oxidation system according to following reactions (Thomas and Vanderschuren 1997, 2000).

The possible NO absorption reactions are:

$$2NO + 2H_2O_2 \rightarrow 2NO_2 + 2H_2O \quad (4)$$

$$2NO_2 + H_2O_2 \rightarrow 2HNO_3 \quad (5)$$

Overall reaction is

$$2NO + 3H_2O_2 \rightarrow 2HNO_3 + 2H_2O. \quad (6)$$

From Fig. 4b, it is evident that NO absorption efficiency increased with increasing H_2O_2 concentration. However, absorption efficiency slightly decreased when increasing H_2O_2 concentration from 0.25 to 2.5 % at higher velocities. Considerable absorption can be seen at H_2O_2 concentration more than 0.7 % and gas velocity <0.06 m/s. Upto ~66 %, absorption was determined at 2 % H_2O_2 concentration and gas velocity 0.02 m/s. Reason may be that at lower velocity, the liquid–gas contact time for bubbles in riser and downcomer of the reactor is more. As the H_2O_2 concentration increases, oxidising ability of media increases which converts NO into NO_2 and further absorbed as a formation of HNO_2 and HNO_3 and therefore, absorption efficiency increases (Thomas and Vanderschuren 1997, 2000).

It can be seen from Fig. 4c that NO absorption efficiency increased with increasing H_2O_2 concentration as well as gas concentration. However, at higher gas velocities, absorption efficiency slightly decreased above H_2O_2 concentration and gas concentration of 2 % and 2,500 ppm, respectively. The liquid–gas reaction time is lower at higher gas velocities leading to lower absorption. Substantial absorption was observed at H_2O_2 concentration more than 0.7 % and gas concentration more than 1,500 ppm. Further, it is evident that from this figure plotted at gas velocity 0.065 m/s that gas velocity plays an important role in NO absorption, since lower absorption can be obtained at this velocity as compared to values seen from Fig. 5a, b. Therefore, it is concluded from Fig. 4a–c that range of variables for significant NO absorption was gas velocity less than 0.06 m/s, NO concentration more than 700 ppm and H_2O_2 concentration more than 1.5 %.

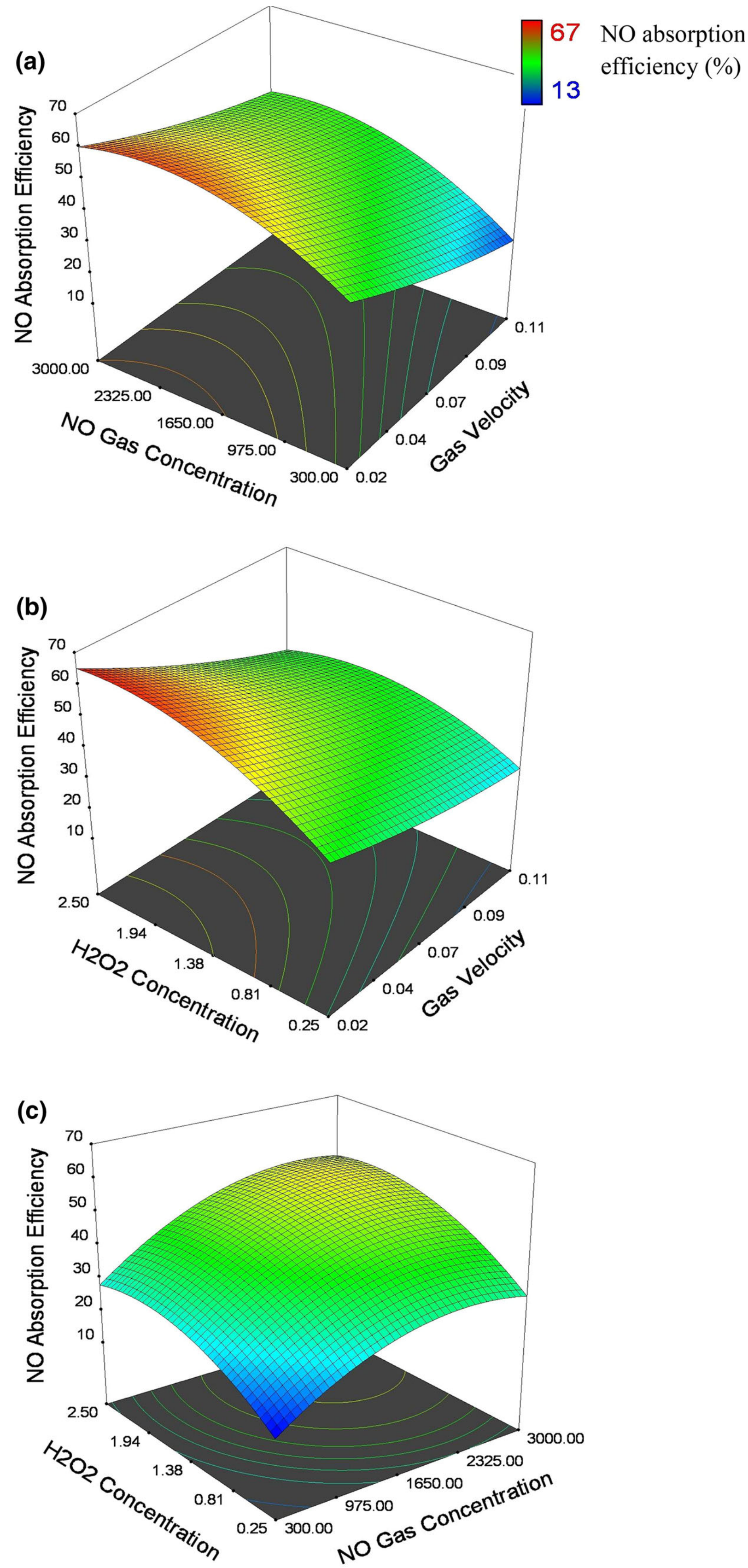

Fig. 4 The 3D plots showing effect of two independent variables (other variables were held at their respective centre levels): **a** Inlet NO gas concentration (ppm) and gas velocity (m/s), **b** H_2O_2 concentration (%) and gas velocity (m/s), **c** H_2O_2 concentration (%) and inlet NO gas concentration (ppm)

At higher concentration of NO in bulk gas, concentration gradient is larger, thus improving mass transfer from gas to liquid phase through conversion of NO to nitrate. The results show that the volumetric mass transfer coefficient (KLa) and the rate of absorption coefficient (RA) increase with the superficial gas velocity. With increase in superficial gas velocity, gas hold-up and turbulence of the system increases which subsequently increases the values of KLa and RA. Maximum value of KLa and RA was estimated to be 9.2×10^{-3} L/s and 6.05×10^{-6} mol/L s, respectively, at superficial gas velocity 0.06 m/s. According to Marquez et al. (1999), hydrodynamics, gas/liquid mass transfer and chemical reaction in an external loops gas-lift reactor for the fast, reactive absorption of carbon dioxide (CO_2) into aqueous potassium hydroxide (KOH) are coupled. The phenomena can be described by a pseudo-steady-state model. Similarly, in this case rapid absorbing, characteristics of NO in H_2O_2 may be following pseudo-steady-state model for interactions of hydrodynamics, mass transfer and chemical reaction for the bubbly flow regime in the riser.

Further, to evaluate the interactive effects of the studied independent variables on NO absorption for all combinations under study, perturbation graphs were drawn and depicted in Fig. 5. The perturbation plots illustrate responses as each independent variable moves from the preferred reference with all other variables held constant at the middle of the design space (the coded zero level). As illustrated by the perturbation plots in Fig. 5, all three independent variables (NO gas velocity, gas concentration and H_2O_2 concentration) have an influence on the NO absorption process of studied combinations. The curve with the most prominent change was the perturbation curve of NO gas velocity compared to those of the other independent variables fixed at their maximum levels. Thus, NO gas velocity was the most significant factor that contributed to the removal of NO by the H_2O_2 absorption process.

Optimisation results showed that the coded values of NO gas velocity, gas concentration and H_2O_2 concentration at optimum condition were x_1, -1; x_2, 0.441 and x_3, 0.644, respectively, to achieve maximum NO absorption efficiency (67.8 %). The optimum actual values for three operating variables, considered using specific experimental setup in this study, were NO gas velocity, 0.02 m/s; gas concentration, 2,246 ppm and H_2O_2 concentration, 2.1 %. The liquid solution analysed for nitrate formed in the solution. Since the experiments are conducted in semi-batch mode for 120 min, the concentration of HNO_3 at the end of experiments obtained was [HNO_3] 0.0002 M at gas velocity, 0.02 m/s; gas concentration, 300 ppm; H_2O_2 concentration, 0.25 % and [HNO_3] 0.062482 M at gas velocity, 0.11 m/s; gas concentration, 3,000 ppm; H_2O_2 concentration, 2.5 %.

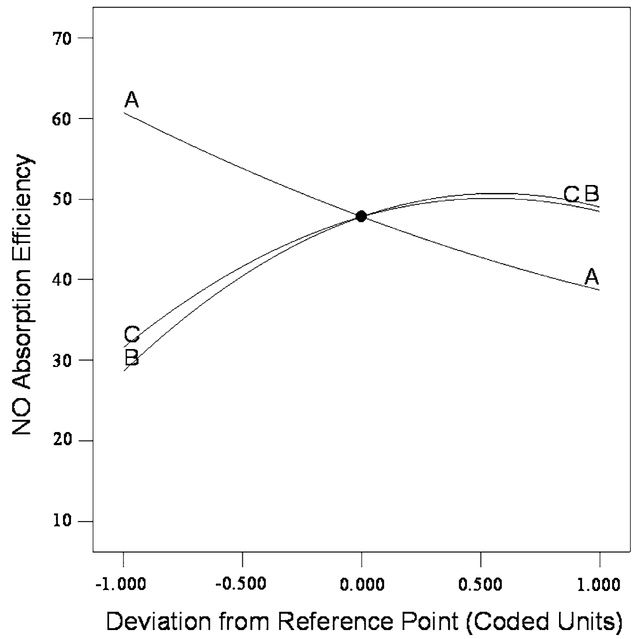

Fig. 5 Overlay plot perturbation of independent variables on NO absorption efficiency. Experimental conditions: **A** Gas velocity = 0.065 m/s, **B** NO gas concentration = 1,650 ppm, **C** H_2O_2 concentration = 1.38 %

Model validation studies

In order to verify the validity of proposed regression, additional nine sets of experiments were conducted for different combinations of the three independent process variables in a random fashion, each within its respective experimental range, and corresponding response variable (absorption efficiency, %) was generated using the uncoded values of the process variables and model Eq. (3). Table 5 presents the experimental conditions along with the model predicted and experimental results. Experimentally determined response factor values for each of the nine sets of process variables were then used along with the model predicted values to compute the R^2 value. A high correlation ($R^2 = 0.957$) among the predicted and the measured values of the response factor suggests for the adequacy of the proposed quadratic model in predicting the response variable for the validation data set comprised of different combinations of the process variables. Under optimum conditions, the experimental NO absorption efficiency was found to be 64.6 %, which is very close to the value by the proposed model (Table 5). Maximum absorption efficiency of NO, obtained in single-stage ALR at NO gas velocity, 0.02 m/s; gas concentration, 2,246 ppm; H_2O_2 concentration, 2.1 % and temperature, 30 °C may be improved by using two-stage ALR.

Further, to examine whether the experimental absorption data in validation set differ from the corresponding model predicted values of the response variable, a nonparametric

Mann–Whitney U test was conducted, which is based on the combined ranking of the two samples and summing up their total rank scores (U) separately after their break up. An expected score value is determined as (Hamilton and Mann-Whitney 2004),

$$E(U) = \frac{n_U(N+1)}{2} \tag{7}$$

where $E(U)$ is the expectation of U, n_U is the sample size of the data set being tested, and N is the total number of samples ($N = n_1 + n_2$). A z-score under the normal curve is then calculated as (Hamilton and Mann-Whitney 2004),

$$z = \frac{U_{\max} - E(U)}{\sqrt{n_1 n_2 (N+1)/2}} \tag{8}$$

where $U_{\max}$ is the maximum total rank score value, and n_1 and n_2 are the sample sizes of the two independent data sets. The z-score for the present validation data set determined to be 0.1324 and the two-tailed probability associated with this z-score obtained as $p = 0.894$, which is greater than the chosen probability level of $p = 0.05$, suggesting there was an insignificant difference between the measured and the model predicted responses in validation set (Singh et al. 2011).

Besides, a parametric two-sample (unpaired) t test was also performed to evaluate the relationship between the model predicted and the experimental responses, as well as to prove model results. The Box-and-Whisker plot shown in Fig. 6a suggests that both distributions are close enough to normal to use a parametric hypothesis such as a two-sample t test, as suggested by Hamilton (2004). Since, both the predicted and experimental data sets have almost equal variance; the standard error of the two sets can be pooled as (Hamilton 2004);

Table 5 Experimental conditions for model validation with corresponding predicted and observed responses

Additional experiment no.	Gas velocity (m/s)	Gas conc. (ppm)	H_2O_2 conc. (%)	Predicted NO efficiency (%)	Experimental NO efficiency (%)
1	0.06	3,000	1.3	49.39	51.4
2	0.06	1,650	0.25	32.42	34.6
3	0.06	1,650	2.5	50.16	47.3
4	0.1	1,700	1.35	40.7	38.9
5	0.105	300	1.0	16.7	18.2
6	0.06	333	3.0	25.63	23.3
7	0.06	3,000	3.0	48.38	44.1
8	0.06	2,000	0.5	39.22	40.1
9	0.04	3,000	1.35	54.53	57.5
Optimum condition	0.02	2,246	2.1	67.8	64.6

$$se_p = \frac{s_1 + s_2}{2}\sqrt{\frac{1}{n_1} + \frac{1}{n_2}} \tag{9}$$

where se_p is the pooled standard error, s_1 and s_2 are the standard deviations, and n_1 and n_2 are the sample sizes of the two data sets. The t test statistics was applied for determination of t_{cal}-value as (Hamilton 2004):

$$t_{cal} = \frac{\overline{y_1} - \overline{y_2}}{se_p} \tag{10}$$

where t_{cal} is the calculated t statistics, and $\overline{y_1}$ and $\overline{y_2}$ are the mean values of the independent data sets. The value was compared with the tabulated t value (t_{tab}) for the corresponding degrees of freedom. The calculated t value ($t_{\mathrm{cal}} = 0.0321$) was found to be less than the tabulated t value ($t_{\mathrm{tab}} = 2.12$), suggesting that there is insignificant statistical difference between the two set of independent samples. Therefore, both the nonparametric Mann-Whitney test and the two-sample t statistics concluded with 95 % certainty that the proposed quadratic model provided a satisfactory fit to the additional experimental data set for validation (Singh et al. 2011), as also seen in Fig. 6b.

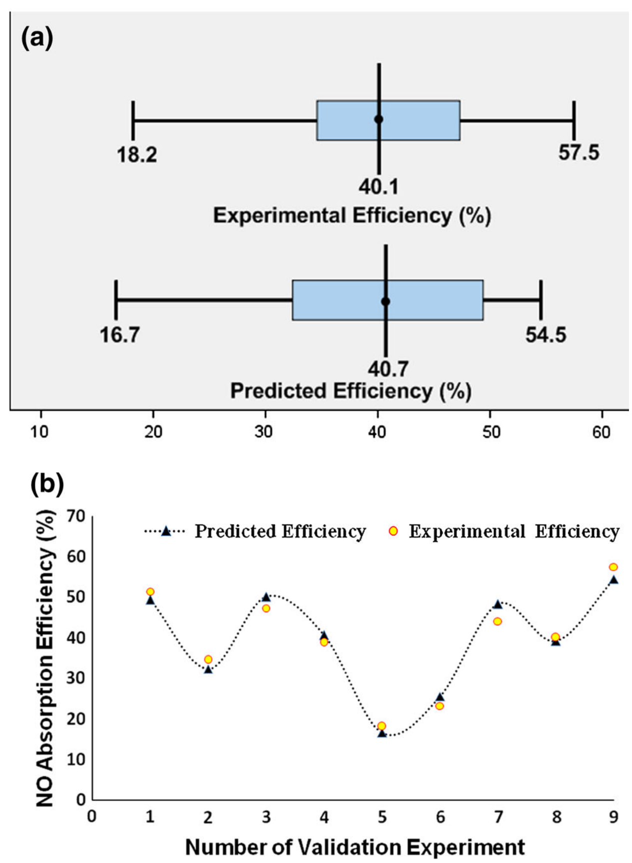

Fig. 6 Comparison between additional validation experimental results and predicted responses **a** Box–Whisker plot and **b** Agreement between two independent samples

Conclusion

The study was taken with the aim of finding the feasibility of H_2O_2 for maximum absorption of NO gas in bench scale ALR using response surface methodological approach, which proves to be very effective and time saving technique for studying the influence of major process parameters on the response factor by significantly reducing the number of experiments and further facilitating the optimum conditions. A regression model was proposed to describe the influence of independent variables and their interactions on NO absorption rate. ANOVA analysis indicated the proposed regression model based on Box–Behnken design agreed with the experimental case with R^2 and R^2_{adj} correlation coefficients of 0.983 and 0.954, respectively. The estimated optimum conditions from the proposed regression model applicable for reactor in the present study for NO absorption at 30 °C temperature were NO gas velocity, 0.02 m/s, NO gas concentration, 2,246 ppm and H_2O_2 concentration, 2.1 %, respectively, where $\sim$68 % of absorption could be obtained which was confirmed with the experimental value. NO gas velocity was the most significant component of the quadratic model for the present absorbent-absorbate system. The model validation results suggested the adequacy of the developed model for its application to new data sets. This study clearly confirmed that Box–Behnken design combined with response surface methodology and optimisation can efficiently be applied to analyse NO absorption data in ALR to understand the relationships among the independent and response variables and to maximise the absorption efficiency.

Acknowledgments The authors are thankful to the Director, National Environmental Engineering Research Institute, Nagpur (India) for his encouragement and guidance to publish this work.

References

Ahmad AL, Ismail S, Bhatia S (2005) Optimization of coagulation-flocculation process for palm oil mill effluent using response surface methodology. Environ Sci Technol 39:2828–2834

Can MY, Kaya Y, Algur OF (2006) Response surface optimization of the removal of nickel from aqueous solution by cone biomass of *Pinus sylvestris*. Bioresour Technol 97:1761–1765

Evans M (2003) Optimization of manufacturing processes: a response surface approach. Maney Publishing, London

Fadavi A, Chisti Y (2005) Gas–liquid mass transfer in a novel forced circulation loop reactor. Chem Eng J 112:73–80

Guo C, Stine KJ, Kauffman JF, Doub WH (2008) Assessment of the influence factors on in vitro testing of nasal sprays using Box–Behnken experimental design. Euro J Pharm Sci 35:417–426

Hamilton MJ (2004) 2 Sample t-test (1 tailed equal variance). Department of Anthropology, University of New Mexico, Albuqueque

Hamilton MJ, Mann-Whitney U (2004) 2 sample test (a. k. a. Wilcoxon Rank Sum Test). Department of Anthropology, University of New Mexico, Albuqueque

Han PF, Tang LX, Huang YQ, Ouyang PK (2005) Experimental study on the hydrodynamics and mass transfer characteristics of ultrasonic loop airlift reactor. Can J Chem Eng 83:204–211

Jia X, Wen J, Jiang Y, Liu X, Feng W (2006) Modeling of batch phenol biodegradation in internal loop airlift bioreactor with gas recirculation by *Candida tropicalis*. Chem Eng Sci 61: 3463–3475

Jin DS, Deshwal BR, Park YS, Lee HK (2006) Simultaneous removal of SO_2 and NO by wet scrubbing using aqueous chlorine dioxide solution. J Hazard Mater B 135:412–417

Kasper JM, Clausen CA, Cooper CD (1996) Control of nitrogen oxide emissions by hydrogen peroxide enhanced gas-phase oxidation of nitric oxide. J Air Waste Manage Assoc 46:127–133

Khajeh M (2011) Optimization of process variables for essential oil components from Satureja hortensis by supercritical fluid extraction using Box–Behnken experimental design. J Supercrit Fluids 55:944–948

Kockal N, Ozturan T (2011) Optimization of properties of fly ash aggregates for high-strength lightweight concrete production. Mater Design 32:3586–3593

Liu HL, Lan YW, Cheng YC (2004) Optimal production of sulphuric acid by *Thiobacillus thiooxidans* using response surface methodology. Process Biochem 39:1953–1961

Long X, Xin Z, Chen M, Li W, Xiao W, Yuan W (2008) Kinetics for the simultaneous removal of NO and SO_2 with cobalt ethylenediamine solution. Sep Purif Technol 58:328–334

Marquez MA, Amend RJ, Carbonell RG, SaHez AE, Roberts GW (1999) Hydrodynamics of gas-lift reactors with a fast, liquid-phase reaction. Chem Eng Sci 54:2263–2271

Martendal E, Budziak D, Carasek E (2007) Application of fractional factorial experimental and Box–Behnken designs for optimization of single drop microextraction of 2,4,6-trichloroanisole and 2,4,6-tribromoanisole from wine samples. J Chromatogr A 1148:131–136

Mehrnia MR, Jafar T, Bonakdarpour B, Akbarnejad MM (2005) Gas hold-up and oxygen transfer in a draft-tube airlift bioreactor with petroleum-based liquids. Biochem Eng J 22:105–110

Moghaddam SS, Moghaddam MRA, Arami M (2011) Response surface optimization of acid red 119 dye from simulated wastewater using Al based waterworks sludge and polyaluminium chloride as coagulant. J Environ Manage 92:1284–1291

Montgomery DC (1996) Design and analysis of experiments, 4th edn. Wiley, USA

Murthy MSRC, Swaminathan T, Rakshit KY (2000) Statistical optimization of lipase catalyzed hydrolysis of methyloleate by response surface methodology. Bioprocess Eng 22:35–39

Myers RH, Montgomery DC (2002) Response surface methodology: process and product optimization using designed experiments, 2nd edn. Wiley, New York

Noordin MY, Venkatesh VC, Sharif S, Elting S, Abdullah A (2004) Application of response surface methodology in describing the performance of coated carbide tools when turning AISI 1045 steel. J Mater Process Technol 145:46–58

Paiva JL, Kachan GC (1998) Modeling and simulation of a packed column for NOx absorption with hydrogen peroxide. Ind Eng Chem Res 37:609–614

Singh KP, Gupta S, Singh AK, Sinha S (2011) Optimizing adsorption of crystal violet dye from water by magnetic nanocomposite using response surface modeling approach. J Hazard Mater 186:1462–1473

Thomas D, Vanderschuren J (1997) Modeling of NOx absorption into nitric acid solutions containing hydrogen peroxide. Ind Eng Chem Res 36:3315–3322

Thomas D, Vanderschuren J (1998) Effect of temperature on NOx absorption into nitric acid solutions containing hydrogen peroxide. Ind Eng Chem Res 37:4418–4423

Thomas D, Vanderschuren J (2000) Analysis and prediction of liquid phase composition for absorption of nitrogen oxides into aqueous solutions. Sep Purif Technol 18:37–45